する患者へのリスクについては、対象疾患を治療することによる患者へのベネフィット等とのバランスを踏まえて合理的に評価すること）。

7　製造工程で外来遺伝子の導入が行われ、最新の知見に基づき、最終製品中で機能している場合や残存していると判断された場合には、遺伝子治療用医薬品指針に定めるところに準じて試験を行うこと。特に、ウイルスベクターを使用した場合には増殖性ウイルスがどの程度存在するかを検査するとともに、検査方法が適切であることについても明らかにすること。

また、導入遺伝子及びその産物の性状について調査し、安全性について明らかにすること。細胞については、増殖性の変化、良性腫瘍を含む腫瘍形成及びがん化の可能性について考察し、明らかにすること。染色体への挿入の可能性があるベクターを用いた場合には、挿入変異による細胞の異常増殖性や造腫瘍性についての評価や臨床適応に当たっての長期フォローアップの必要性を考慮すること。

8　動物由来のモデル製品を含めて製品の入手が容易であり、かつ臨床上の適用に関連する有用な安全性情報が得られる可能性がある場合には、合理的に設計された一般毒性試験の実施を考慮すること。

なお、一般毒性試験の実施に当たっては、平成元年9月11日付け薬審1第24号厚生省薬務局新医薬品課長・審査課長連名通知「医薬品の製造(輸入)承認申請に必要な毒性試験のガイドラインについて」の別添「医薬品毒性試験法ガイドライン」等を参照すること。

第５章　ヒトES細胞加工医薬品等の効力又は性能を裏付ける試験

1　技術的に可能かつ科学的に合理性のある範囲で、実験動物又は細胞等を用い、適切に設計された試験により、ヒトES細胞加工医薬品等の機能発現、作用持続性及び医薬品・医療機器として期待される臨床効果の実現可能性(Proof-of-Concept)を示すこと。

2　遺伝子導入細胞にあっては、導入遺伝子からの目的産物の発現効率及び発現の持続性、導入遺伝子の発現産物の生物活性並びに医薬品等として期待される臨床効果の実現可能性(Proof-of-Concept)を示すこと。

3　適当な動物由来細胞・組織製品モデル又は疾患モデル動物がある場合には、それを用いて治療効果を検討すること。

4　治験開始段階では、当該製品の効力又は性能による治療が他の治療法と比較したときはるかに優れて期待できることが国内外の文献又は知見等により合理的に明らかにされている場合には、必ずしも詳細な実験的検討は必要とされない。

第６章　ヒトES細胞加工医薬品等の体内動態

1　製品を構成する細胞・組織及び導入遺伝子の発現産物について、技術的に可能で、かつ、科学的合理性がある範囲で、実験動物での吸収及び分布等の体内動態に関する試験等により、患者等に適用された製品中の細胞・組織の生存期間、効果持続期間を推測し、目的とする効果が十分得られることを明らかにすること（注：体内動態に関する試験等には、例えば組織学的検討、AluPCR法、磁気共鳴画像診断法(MRI)、陽電

子放射断層撮影法(PET)、単一光子放射断層撮影法(SPECT)、バイオイメージングなどがある）。

2　ヒトES細胞加工医薬品等の用法（投与方法）について、動物実験を通してその合理性を明らかとすること。特に、全身投与にあっては投与後の細胞の全身分布を動物実験などから外挿し、有用性の観点から議論すること（注:投与経路ごとにどこに生着するかは不明であるが、全身投与よりも局所投与が望ましいと想定される。しかし、全身投与であってもその有用性において被投与患者に有益であると合理的に説明が可能である場合には用法として設定可能である。例えば、生着を期待する臓器以外への分布を最低限に抑えることが合理的な投与方法であると想定される。また、異所性生着しても、被投与患者にとって不利益（生体機能への悪影響）が生じない場合は用法として肯定できる可能性がある。異所性分化による不利益とは、例えば当該細胞が心臓に異所性生着して骨形成する場合が想定され、それが不整脈を惹起したような場合である）。

3　当該細胞・組織が特定の部位(組織等)に直接適用又は到達して作用する場合には、その局在性を明らかにし、局在性が製品の有効性・安全性に及ぼす影響を考察すること。

第７章　臨床試験

ヒトES細胞加工医薬品等の臨床試験を開始するに当たって支障となる品質及び安全性上の問題が存在するか否かの段階においては、臨床上の有用性を勘案して評価されるものであり、ヒトES細胞加工医薬品等について予定されている国内の臨床試験計画について以下の項目を踏まえて評価すること。その際、明らかに想定される製品のリスクを現在の学問・技術を駆使して排除し、その科学的妥当性を明らかにした上で、なお残る「未知のリスク」と、重篤で生命を脅かす疾患、身体の機能を著しく損なう疾患、身体の機能や形態を一定程度損なうことによりQOLを著しく損なう疾患などに罹患し、従来の治療法では限界があり、克服できない患者が「新たな医療機会を失うことにより被るかもしれないリスク」とのリスクの大小を勘案し、かつ、これらすべての情報を開示した上で患者の自己決定権に委ねるという視点を持つこと、すなわち、リスク・期待されるベネフィットの情報を開示した上で臨床試験に入るかどうかの意思決定は患者が行うという視点を入れて評価することが望まれる。

1　対象疾患

2　対象とする被験者及び除外すべき被験者の考え方

3　ヒトES細胞加工医薬品等及び併用薬の適用を含めた、被験者に対して行われる治療内容（注：投与・移植した細胞の機能を維持・向上・発揮させるために併用する薬剤が想定される場合、当該薬剤の作用を *in vitro* あるいは *in vivo* で検証すること）。

4　既存の治療法との比較を踏まえた臨床試験実施の妥当性

5　現在得られている情報から想定される製品並びに患者のリスク及びベネフィットを含め、被験者への説明事項の案

なお、臨床試験は、適切な試験デザイン及びエンドポイントを設定して実施する必要があり、目的とする細胞・組織の由来、対象疾患及び適用方法等を踏まえて適切に

計画すること。

厚生労働科学研究費補助金（再生医療実用化研究事業）
分担研究報告書

「関節軟骨病変に対する自己滑膜間葉系幹細胞由来三次元人工組織移植法」の産業化支援に関する研究

研究分担者　辻　紘一郎　株式会社ツーセル　代表取締役社長

研究要旨
「関節軟骨病変に対する自己滑膜間葉系幹細胞由来三次元人工組織移植法」を、厚生労働省の定める先進医療へスムーズに移行させるために、「滑膜幹細胞を原材料とする軟骨移植材（ｇMSC)」の薬事戦略相談の実施、調査、検討した。

A.研究目的
滑膜由来間葉系幹細胞（MSC）を用いた再生医療のレギュラトリーサイエンスについて、国内外の情報を収集、解析をし、「関節軟骨病変に対する自己滑膜間葉系幹細胞由来三次元人工組織移植法」の実用化を薬事戦略を軸として目指す。

B.研究方法
薬事戦略相談「滑膜幹細胞を原材料とする軟骨移植材（ｇMSC)」の事前相談を計３回、厚生労働省医薬食品局、厚生労働省医政局への相談を計２回実施した。また、国際学会「World Stem Cell　Summit 2012」(米国・フロリダ)などで再生医療の臨床について調査を行った。

C.研究結果
「滑膜幹細胞を原材料とする軟骨移植材（ｇMSC)」の薬事戦略相談の事前相談および厚生労働省医政局との打ち合わせを複数回繰り返し、仕様、デザイン、設計に係る試案の実現性調査と、必要な試験・治験に関する指導・助言を受け情報収集が行えた。

D.考察
情報収集の結果、再生医療の実施において求められる基本要素（受け入れや規制）はほぼ同一であり、これにいかに申請ごとに異なる事例を盛り込んでいくかが重要かと思われた。

E.結論
申請ごとに異なる事例を調査し反映させることが重要である。再生医療をスムーズに実用化させるには、申請ごとにことなる事例を「事例集」として公表する制度が必要と考える。

F.研究発表
１．論文発表
なし
２．研究発表
辻　紘一郎「再生医療の事業化－有血清培養から無血清培養へ、自家移植からの他家（同種）移植へ」第 12 回日本再生医療学会総会　パネルディスカッション「スーパー特区の成果と課題」(2013.03)

I.知的財産権の出願・登録状況
なし

厚生労働科学研究費補助金（再生医療実用化研究事業）
分担研究報告書

外科的移植手技の開発・改良

研究分担者　堀部　秀二　大阪府立大学　総合リハビリテーション　教授

研究要旨

ＴＥＣの移植に際しては、脱落の予防のためＴＥＣを移植部位に一定時間静置する必要がある。通常の関節鏡手術では視野の確保のため関節内を液体で満たし作業を行うが、ＴＥＣ移植の際には、その水流により脱落の恐れがある。そこで、安定しかつ低侵襲なＴＥＣの移植手技の確立を目的とした調査を行った。

A．研究目的

ＴＥＣの移植の際の手術手技の確立のための調査・検討を行なうことである。

B．研究方法

国内外の関節鏡視下細胞治療の現状把握並びに情報交換を行った。

その結果を踏まえ、関節鏡手術の際に、腹腔鏡手術等でも使用される二酸化炭素ガス還流下におけるＴＥＣの移植が可能か検討した。

（倫理面への配慮）

ヘルシンキ宣言に基づく倫理的原則に留意、「ヒト幹細胞を用いる臨床研究に関する指針」を遵守した。

C．研究結果

20l/minの還流速度による二酸化炭素ガスの関節内の充満により、ＴＥＣ移植の際に必要な視野、および作業空間が確保できることを確認できた。

D．考察

二酸化炭素ガスの使用により、低侵襲かつ確実なＴＥＣの移植が可能となる可能性が示唆された。

E．結論

二酸化炭素ガス還流を用いた関節鏡手術によりＴＥＣをより低侵襲で移植できる可能性が示された。

F．健康危険情報

特になし

G．研究発表

1.　論文発表

・Kita, K., **S. Horibe**, K. Shino et.al. (2012) Effects of medial patellofemoral ligament reconstruction on patellar tracking. *Knee Surg Sports Traumatol Arthrosc,* 20, 829-37.

・Takao, R., H. Oguro, **S. Horibe** et. al.(2012a) Epidemiological study of the relationship between C-reactive protein and diabetes in Japanese females. *生物試料分析,* 35, 420-425.

・Takao, R., H. Oguro, **S. Horibe** et. al.(2012) Epidemiology Study into the Connection Between C-Reactive Protein and Dyslipidemia (C反応性蛋白と脂質異常症の関連性についての疫学研究). *医学と生物学,* 156, 585-591.

・Tanaka, Y., K. Shino, **S. Horibe**, et.al. (2012) Triple-bundle ACL grafts evaluated by second-look arthroscopy. *Knee Surg Sports Traumatol Arthrosc,* 20, 95-101.

・Tsujii, A., Y. Tanaka, **S. Horibe** et. al. (2012) Knee hemarthrosis after arthroscopic surgery in an athlete with low factor XIII activity. *Sports Med Arthrosc Rehabil Ther Technol,* 4, 35.

・Uchida, R., Y. Toritsuka, S. Horibe et.al.(2012) Chondral fragment of the lateral femoral trochlea of the knee in adolescents. *Knee,* 19, 719-23

・Yonetani, Y., Y. Tanaka, **S. Horibe** et.al. (2012) Transarticular drilling for stable juvenile osteochondritis dissecans of the medial femoral condyle. *Knee Surg Sports Traumatol Arthrosc,* 20, 1528-32.
・**堀部, 秀二**、田中, 美成、米谷, 泰一　他 (2012) 【アスリートの半月板損傷-治療の選択、リハビリテーションとスポーツ復帰-】 アスリートに対する半月板治療の選択 外側半月板損傷を中心に. *臨床スポーツ医学,* 29, 995-999.
・**堀部 秀二**、田中 美成、米谷 泰一　他 (2012)【臨床現場に必要な運動器画像診断入門】 膝スポーツ傷害の画像診断. *MEDICAL REHABILITATION*, 163-172.

2.　学会発表
ESSKA Congress (2012.5, Geneva)
JOA 2012 (2012.5, 京都)
JOSKAS2012 (2012.7, 沖縄)

H．知的財産権の出願・登録状況
特になし

研究成果の刊行に関する一覧表

雑誌

発表者氏名	論文タイトル名	発表誌名	巻号	ページ	出版年
Ando W	Detection of abnormalities in the superficial zone of cartilage repaired using a tissue engineered construct derived from synovial stemcells.	European Cells and Materials	24	292-307	2012
Yoshida K	Treatment of Partial Growth Arrest Using an In Vitro-generated Scaffold-free Tissue-engineered Construct Derived From Rabbit Synovial Mesenchymal Stem Cells.	J Pediatr Orthop.	32(3)	314-21	2012
Ando W	Ovine synovial membrane-derived mesenchymal progenitor cells retain the phenotype of the original tissue that was exposed to in-vivo inflammation: evidence for a suppressed chondrogenic differentiation potential of the cells.	Inflamm Res.	61(6)	599-608	2012
Oya K	Morphological Observations of Mesenchymal Stem Cell Adhesion to a Nanoperiodic-Structured Titanium Surface Patterned Using Femtosecond Laser Processing	Jpn. J. Appl. Phys.	51	125203-1-7	2012
Akamine, Y	Prolonged matrix metalloproteinase-3 high expression after cyclic compressive load on human synovial cells in three-dimensional cultured tissue.	Int J Oral Maxillofacial Surg	41	874-881	2012
Akiyama, K.	Three- dimensional distribution of articular cartilage thickness in the elderly talus and calcaneus analyzing the subchondral bone plate density.	Osteoarthritis Cartilage	20	296-304	2012
Kawato, Y	Nkx3.2 promotes primary chondrogenic differentiation by upregulating col2a1 transcription.	PLoS One	7	e34703	2012
Lee, DS	Efficient modification of the surface properties of interconnected porous hydroxyapatite by low-pressure low-frequency plasma treatment to promote its biological performance.	Journal of Physics D, Applied Physics	45	372001	2012

Oze, H.	Impact of medium volume and oxygen concentration in the incubator on pericellular oxygen concentration and differentiation of murine chondrogenic cell culture.	In Vitro Cell Dev Biol Anim	48	123-230	2012
Satoru Sasagawa	SIK3 is essential for chondrocyte hypertrophyduring skeletal development in mice	Development	139 (6)	1153-63	2012
Yamasaki, N.	Hypoxia favors maintenance of the vascular smooth muscle cell phenotype in culture.	Journal of Biochemical and Molecular Toxicology	26	381-383	2012
吉川秀樹	人工骨による骨再生	化学工業	63	504-509	2012
Tetsuo Minamino	Design and rationale of low-dose erythropoietin in patients with ST-segment elevation myocardial infarction (EPO-AMI-II study): A randomized controlled clinical trial.	Cardiovascular Drugs and Therapy	26	409-416	2012
Shudo Y	Myocardial Layer-Specific Effect of Myoblast Cell-Sheet Implantation Evaluated by Tissue Strain Imaging.	Circ J.			2012
Miki K	Bioengineered myocardium derived from induced pluripotent stem cells improves cardiac function and attenuates cardiac remodeling following chronic myocardial infarction in rats.	Stem Cells Translate. Med.	1(5)	430-437	2012
Kawamura M	Feasibility, safety, and therapeutic efficacy of human induced pluripotent stem cell-derived cardiomyocyte sheets in a porcine ischemic cardiomyopathy model.	Circulation.	**126**(11 Suppl 1)	S29-37	2012
Uchinaka A	Transplantation of elastin-secreting myoblast sheets improves cardiac function in infarcted rat heart.	Mol Cell Biochem.	**368**(1-2)	203-14	2012
Saito S	Myoblast sheet can prevent the impairment of cardiac diastolic function and late remodeling after left ventricular restoration in ischemic cardiomyopathy.	Transplantation.	**93**(11)	1108-15	2012
Kazuo Takayama	Generation of metabolically functioning hepatocytes from human pluripotent stem cells by FOXA2 and HNF1a transduction	Journal of Hepatology	57	628–636	2012
Mariko Moriyama	Human adipose tissue-derived multilineage progenitor cells exposed to oxidative stress induce neurite outgrowth in PC12 cells through p38 MAPK signaling	Journal of Hepatology,	13:21,	628–636	2012
Morikawa T	Suppressive effects of coumarins from Mammea siamensis on inducible nitric oxide synthase expression in RAW264.7 cells.	Bioorg Med Chem.	20(16)	4968-77	2012

Yosuke Mitsui	Comparative studies on glycoproteins expressing polylactosamine-type N-glycans cancer cells	Journal of Pharmaceutical and Biomedical Analysis	70	718– 726	2012
Kazuo Takayama	Efficient Generation of Functional Hepatocytes From Human Embryonic Stem Cells and Induced Pluripotent Stem Cells by HNF4α Transduction	Molecular Therapy	20 no. 1	127–137,	2012
Nagamoto Y	The promotion of hepatic maturation of human pluripotent stem cells in 3D co-culture using type I collagen and Swiss 3T3 cell sheet	Biomaterials.	33(18)	4526-34.	2012
Fukushima E	Partial filling affinity capillary electrophoresis using large-volume sample stacking with an electroosmotic flow pump for sensitive profiling of glycoprotein-derived oligosaccharides.	J Chromatogr A.	13	84-9	2012
Eiki Maeda	Analysis of Nonhuman N-Glycans as the Minor Constituents in Recombinant Monoclonal Antibody Pharmaceuticals	Anal. Chem	84	2373–2379	2012
Morikawa T	Anti-hyperlipidemic constituents from the bark of Shorea roxburghii.	J Nat Med.	66(3)	516-24	2012
Chaipech S	Structures of two new phenolic glycosides, kaempferiaosides A and B, and hepatoprotective constituents from the rhizomes of Kaempferia parviflora.	Chem Pharm Bull	60(1)	1-8	2012
Morikawa T	Antidiabetogenic oligostilbenoids and 3-ethyl-4-phenyl-3,4-dihydroisocoumarins from the bark of Shorea roxburghii.	Bioorg Med Chem.	15;20(2)	832-40	2012
Chaipech S	New flav-3-en-3-ol glycosides, kaempferiaosides C and D, and acetophenone glycosides, kaempferiaosides E and F, from the rhizomes of Kaempferia parviflora.	J Nat Med.	66(3)	486-92	2012
Yagi Y	Specific detection of N-glycolylneuraminic acid and Galα1-3Gal epitopes of therapeutic antibodies by partial-filling capillary electrophoresis	Original Research Article Analytical Biochemistry	Volume 431, Issue 2, 15	120-126	2012
Katsuhisa Tashiro	Promotion of hematopoietic differentiation from mouse induced pluripotent stem cells by transient HoxB4 transduction	Stem Cell Research	8	300–311	2012
Takayama K	Efficient Generation of Functional Hepatocytes from Human Embryonic Stem Cells and Induced Pluripotent Stem Cells by HNF4α Transduction.	Mol. Ther.,	20(1)	127-137	2012

Yamada K	One-pot characterization of cancer cells by the analysis of mucin-type glycans and glycosaminoglycans.	Anal Biochem.	421(2)	595-606	2012
Takayama K	3D spheroid culture of hESC/hiPSC-derived hepatocyte-like cells for drug toxicity testing.	Biomaterials	34(7)	1781-9	2012
Kita, K	Effects of medial patellofemoral ligament reconstruction on patellar tracking.	Knee Surg Sports Traumatol Arthrosc	20	829-37	2012
Takao, R.,	Epidemiological study of the relationship between C-reactive protein and diabetes in Japanese females.	生物試料分析	35	420-425	2012
Takao, R	Epidemiology Study into the Connection Between C-Reactive Protein and Dyslipidemia (C反応性蛋白と脂	医学と生物学	156	585-591	2012
Tanaka, Y.	Triple-bundle ACL grafts evaluated by second-look arthroscopy.	Knee Surg Sports Traumatol Arthrosc	20	95-101	2012
Tsujii, A.	Knee hemarthrosis after arthroscopic surgery in an athlete with low factor XIII activity.	Sports Med Arthrosc Rehabil Ther Technol	4	35	2012
Uchida, R.	Chondral fragment of the lateral femoral trochlea of the knee in adolescents.	Knee	19	719-23	2012
Yonetani, Y.	Transarticular drilling for stable juvenile osteochondritis dissecans of the medial femoral condyle.	Knee Surg Sports Traumatol Arthrosc	20	1528-32	2012
堀部, 秀二	アスリートの半月板損傷-治療の選択、リハビリテーションとスポーツ復帰-】 アスリートに対する半月板治療の選択　外側半月板損傷を中心に	臨床スポーツ医学	29	995-999	2012
堀部 秀二	【臨床現場に必要な運動器画像診断入門】膝スポーツ傷害の画像診断.	MEDICAL REHABILITATION,		163-172	2012

DETECTION OF ABNORMALITIES IN THE SUPERFICIAL ZONE OF CARTILAGE REPAIRED USING A TISSUE ENGINEERED CONSTRUCT DERIVED FROM SYNOVIAL STEM CELLS

Wataru Ando[1,2,3], Hiromichi Fujie[4,5], Yu Moriguchi[1], Ryosuke Nansai[4], Kazunori Shimomura[1], David A. Hart[2], Hideki Yoshikawa[1] and Norimasa Nakamura[1,6,7,*]

[1]Department of Orthopaedics, Osaka University Graduate School of Medicine, Suita, Osaka, Japan
[2]McCaig Institute for Bone and Joint Health, Faculty of Medicine, University of Calgary, Calgary, Alberta, Canada
[3]Department of Orthopaedics, Kansai Rosai Hospital, Amagasaki, Hyogo, Japan
[4]Biomechanics Laboratory, Department of Mechanical Engineering, Kogakuin University, Hachioji, Tokyo, Japan
[5]Biomechanics Laboratory, Faculty of System Design, Tokyo Metropolitan University, Hino, Tokyo, Japan
[6]Center for Advanced Medical Engineering and Informatics, Osaka University, Suita, Osaka, Japan
[7]Institute for Medical Science in Sports, Osaka Health Science University, Osaka, Japan

Abstract

The present study investigated the surface structure and mechanical properties of repair cartilage generated from a tissue engineered construct (TEC) derived from synovial mesenchymal stem cells at six months post-implantation compared to those of uninjured cartilage. TEC-mediated repair tissue was cartilaginous with Safranin O staining, and had comparable macro-scale compressive properties with uninjured cartilage. However, morphological assessments revealed that the superficial zone of TEC-mediated tissue was more fibrocartilage-like, in contrast to the middle or deep zones that were more hyaline cartilage-like with Safranin O staining. Histological scoring of the TEC-mediated tissue was significantly lower in the superficial zone than in the middle and deep zones. Scanning electron microscopy showed a thick tangential bundle of collagen fibres at the most superficial layer of uninjured cartilage, while no corresponding structure was detected at the surface of TEC-mediated tissue. Immunohistochemical analysis revealed that PRG4 was localised in the superficial area of uninjured cartilage, as well as the TEC-mediated tissue. Friction testing showed that the lubrication properties of the two tissues was similar, however, micro-indentation analysis revealed that the surface stiffness of the TEC-repair tissue was significantly lower than that of uninjured cartilage. Permeability testing indicated that the TEC-mediated tissue exhibited lower water retaining capacity than did uninjured cartilage, specifically at the superficial zone. Thus, TEC-mediated tissue exhibited compromised mechanical properties at the superficial zone, properties which need improvement in the future for maintenance of long term repair cartilage integrity.

Keywords: Cartilage tissue engineering; animal model; image analysis; mechanical properties; mechanical test; microstructure.

*Address for correspondence:
Norimasa Nakamura
Center for Advanced Medical Engineering and Informatics
Osaka University, 2-2 Yamadaoka, Suita
Osaka 565-0871, Japan
Telephone Number: +81-6-6879-3552
FAX Number: +81-6-6879-3559
E-mail: norimasa.nakamura@ohsu.ac.jp

Introduction

It is widely accepted that injuries to articular cartilage do not usually heal spontaneously due to their avascular surroundings and a variety of approaches have been tested to improve cartilage healing (Buckwalter, 2002; Hunziker, 2002). Among them, stem cell therapy could be a promising option to facilitate regenerative tissue repair. Mesenchymal stem cells (MSCs) have the capability to differentiate into a variety of connective tissue cells including bone, cartilage, tendon, muscle, and adipose tissue (Pittenger *et al.*, 1999). These cells may be isolated from various tissues such as bone marrow, skeletal muscle, synovial membrane, adipose tissue, and umbilical cord blood (De Bari *et al.*, 2001; Jankowski *et al.*, 2002; Lee *et al.*, 2003; Wickham *et al.*, 2003). MSCs isolated from synovial membrane may be well suited for cell-based therapies for cartilage because of the relative ease of their harvest and their strong capability for chondrogenic differentiation (De Bari *et al.*, 2001; Sakaguchi *et al.*, 2005; Ando *et al.*, 2007). Recent implantation studies have reported successful repair of cartilage defects using porcine synovial membrane-derived MSCs (Ando *et al.*, 2007; Koga *et al.*, 2008; Koga *et al.*, 2009).

As a potential MSC-based therapeutic method, we have developed a scaffold-free three-dimensional tissue-engineered construct (TEC) composed of allogenic MSCs derived from the synovium and extracellular matrices (ECMs) synthesised by the cells (Ando *et al.*, 2007; Ando *et al.*, 2008), and demonstrated the feasibility of the resultant TEC to facilitate cartilage repair in a large animal study (Ando *et al.*, 2007). Following implantation for 6 months, TEC efficiently repaired the chondral defects by developing a cartilage-like tissue without the development of any immunologic reaction, regardless of skeletal maturity (Shimomura *et al.*, 2010). However, more detailed observations revealed that more spindle shaped fibroblast-like cells were dominant in the superficial area of the repair tissue and this was not observed in normal cartilage (Ando *et al.*, 2007; Shimomura *et al.*, 2010). Therefore, it is important to evaluate the quality of repaired tissue in more detail, especially in the superficial zone area.

The function of articular cartilage is to support and distribute loads in joints and to minimise friction between opposing articular surfaces by the maintenance of lubrication. The adequate permeability of tissues is also

crucial for maintaining the cartilage by transportation of nutrients to chondrocytes in avascular cartilage (Maroudas *et al.*, 1968). In this regard, it is of significance to evaluate the micro-scaled mechanical properties, which are related to compression, lubrication, and permeability of normal and repair articular cartilage. The micro-scaled mechanical properties of *in vitro* engineered cartilaginous tissues have been investigated (Grad *et al.*, 2012). However, that study did not evaluate the properties of *in vivo* implanted tissue, and there have been no reports specifically on the micro-scaled biomechanical properties of the superficial zone of *in vivo* generated repair cartilage in a large-animal model.

In the present study, we have investigated the detailed structure and micro-mechanical properties of the cartilaginous tissue resulting from treatment with TEC in comparison with those of uninjured articular cartilage in a previously validated porcine model. The findings indicate that the superficial zone of the TEC-mediated repair cartilage is uniquely compromised compared to uninjured cartilage.

Material and Methods

Isolation and expansion of synovial mesenchymal stem cells (MSCs)

MSCs were isolated and expanded as previously reported (Ando *et al.*, 2007). Briefly, porcine synovial membranes were obtained aseptically from the knee joints of two four month old male domestic pigs (cross bred animals: Landrace/Yorkshire/Duroc) post-mortem within 12 h of death in accordance with a protocol approved by the institutional ethics committee. Synovial membrane specimens were taken from the area around the anterior cruciate ligament (ACL) of the knee, rinsed with phosphate buffered saline (PBS), minced meticulously, and digested with 0.4 % collagenase IV (Sigma-Aldrich, St. Louis, MO, USA) in high-glucose Dulbecco's modified Eagle's medium (DMEM; Gibco BRL/Life Technologies, Rockville, MD, USA) for 2 h at 37 °C. After neutralisation of the collagenase by growth medium containing DMEM supplemented with 10 % foetal bovine serum (FBS; HyClone, Logan, UT, USA) and 1 % Penicillin/Streptomycin (Gibco BRL/Life Technologies), the resulting cells were collected by centrifugation, washed with PBS, resuspended in the growth medium, and plated in culture dishes.

For expansion, the cells were cultured in the growth medium at 37 °C in a humidified atmosphere of 5 % CO_2, with the medium replaced once per week. After 15-28 days of primary culture, when the cells reached confluence, they were washed twice with PBS, harvested by treatment with trypsin-EDTA (0.25 % trypsin and 1 mM EDTA: Gibco BRL/Life Technologies) and then replated at 1:3 dilution for the first subculture. Cell passages were continued in the same manner with 1:3 dilution when they reached confluence. Cells at passages 4 to 7 were used in the present studies. Our previous studies indicated that cells cultured using the above-mentioned procedure were composed of mesenchymal stem cells by cell surface phenotyping (Ando *et al.*, 2007), therefore the cells were defined as MSCs in the present study.

Development of a basic TEC from MSCs

MSCs were plated on 6 cm diameter culture dishes at a density of $4.0 \times 10^5/cm^2$ in the growth medium with 0.2 mM ascorbic acid 2-phosphate (Asc-2P; Sigma-Aldrich). Within a day, the cells became confluent. After additional culture durations of 7 days, a monolayer complex of the cultured cells and an ECM synthesised by the cells developed, and this was detached from the substratum by application of shear stress at the cell-substratum interface using gentle pipetting. The detached monolayer complex was left in suspension to form a three-dimensional structure by active tissue contraction. This contracted tissue was termed a basic tissue engineered construct (TEC) (Fig. 1ab) (Ando *et al.*, 2007; Ando *et al.*, 2008).

Implantation of basic TEC into porcine chondral defects *in vivo*

The resultant TEC were prepared as an allograft without any chondrogenic stimulation. Four-month-old female domestic immature pigs (n = 6) were anaesthetised by intramuscular injection of a mixture of ketamine hydrochloride (50 mg/mL and 0.6 mL/kg of body weight) and xylazine (20 mg/mL and 0.3 mL/kg of body weight) and continuous intravenous injection of propofol (10 mg/mL and 8 mL/kg/h). After a medial parapatella incision, the medial femoral condyles of the both knees were exposed with the knee in deep flexion, and partial thickness chondral defects of 8.5 mm in diameter and 1.5-2.0 mm in depth, without penetrating the subchondral bone, were created using an electric router (Proxxon, Niersbach, Germany) and diamond disc grinding (Shofu, Kyoto, Japan). These chondral defects were considered to be comparable with ICRS grade III injury (http://www.cartilage.org/index.php?pid=223&lang=1) which is used in a clinical setting. In 4 of the 6 pigs, the basic TEC – which was left in suspension for up to 12 h until implantation – were implanted into the defect on one side of the knee without suturing (TEC-treated group). On the other side, the defects were left empty (Untreated group). In the other two pigs, the TEC was implanted in the defects on both sides and this group was add to the TEC-treated group (Ando *et al.*, 2007; Shimomura *et al.*, 2010). All animals were immobilised for 7 days with casting and then were allowed free cage activity. They were euthanised under anaesthesia at 6 months after surgery. Each graft site was divided into two parts. One was fixed and used for subsequent paraffin sectioning and histological analysis, and the other was subjected to mechanical testing including compression testing, friction testing, micro indentation testing, and permeability testing. Cylindrical specimens of 4 mm in diameter and 5 mm in depth were extracted for the mechanical tests. For comparison, cylindrically-shaped, uninjured cartilage-subchondral bone specimens of identical size were also extracted at a distance from the repair sites (uninjured group).

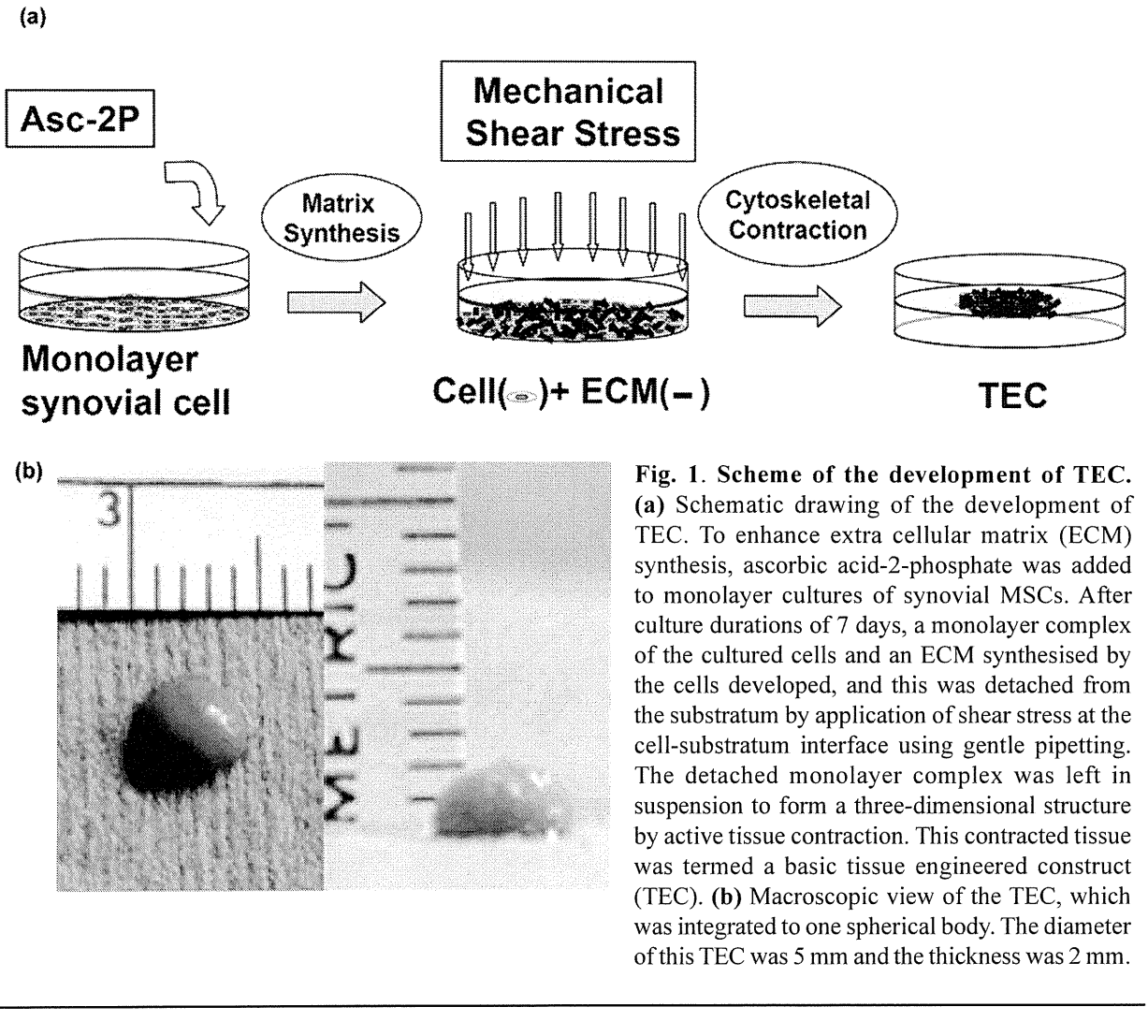

Fig. 1. Scheme of the development of TEC. **(a)** Schematic drawing of the development of TEC. To enhance extra cellular matrix (ECM) synthesis, ascorbic acid-2-phosphate was added to monolayer cultures of synovial MSCs. After culture durations of 7 days, a monolayer complex of the cultured cells and an ECM synthesised by the cells developed, and this was detached from the substratum by application of shear stress at the cell-substratum interface using gentle pipetting. The detached monolayer complex was left in suspension to form a three-dimensional structure by active tissue contraction. This contracted tissue was termed a basic tissue engineered construct (TEC). **(b)** Macroscopic view of the TEC, which was integrated to one spherical body. The diameter of this TEC was 5 mm and the thickness was 2 mm.

Histological and immunohistological analysis

Specimens were fixed with 4 % paraformaldehyde, decalcified with ethylene diamine tetraacetic acid (EDTA), and embedded in paraffin; 4 μm sections were stained with haematoxylin and eosin, as well as Safranin O. The repair tissue was divided into 4 parts of 2 mm width and each area was evaluated using the O'Driscoll scoring system (O'Driscoll, *et al.*, 1988). Each area was also divided into three parts corresponding to the superficial, middle and deep layers and evaluated by several criteria of the O'Driscoll scoring system including cellular morphology, Safranin O staining of the matrix, hypocellularity, and chondrocyte clustering. All scores for each area were averaged.

Picrosirius red was applied to serial sections and observed under polarised light microscopy to assess the collagen fibrils in the superficial layer of the repair tissue.

Serial sections were also subjected to immunohistochemical analysis. A polyclonal antibody (LPN) against proteoglycan 4 (PRG4; lubricin) (Schmidt *et al.*, 2009) was obtained through the courtesy of Dr John Sandy (Rush University, Chicago, IL, USA), and was used as the primary antibody. After the sections were incubated in 0.3 % H_2O_2 in 90 % methanol for 30 min at room temperature to block endogenous peroxidase activity, they were then incubated in 10 % normal goat serum. Next, the antibody LPN was applied to each section, followed by incubation overnight at 4 °C. Detection was then performed using the streptavidin biotin-peroxidase complex technique (Histofine SAB-PO Kit; Nichirei, Tokyo, Japan) before the sections were developed in 3,3-diaminobenzidine tetrahydrochloride (Dojindo Laboratories, Kumamoto, Japan) and counterstained with haematoxylin. Controls included no primary antibody assessments.

Macro-scale quasi-static compression testing

Macro-scale quasi-static unconfined compression testing was performed for each cylindrical specimen using a custom made compression tester (Katakai *et al.*, 2009). The quasi-static compression was applied to the specimen soaked in the saline solution at a rate of 4 μm/s to determine the bulk stiffness of the specimen in the linear region.

Scanning electron microscopy

Some cylindrical specimens were longitudinally sliced in the sagittal plane to yield specimens of 0.3 μm in thickness, using a microtome. Scanning electron microscopic (SEM) analysis was performed for each section specimen using the method developed by Katakai (Katakai, 2008). After dehydration in 50 % ethanol for 5 min, each specimen

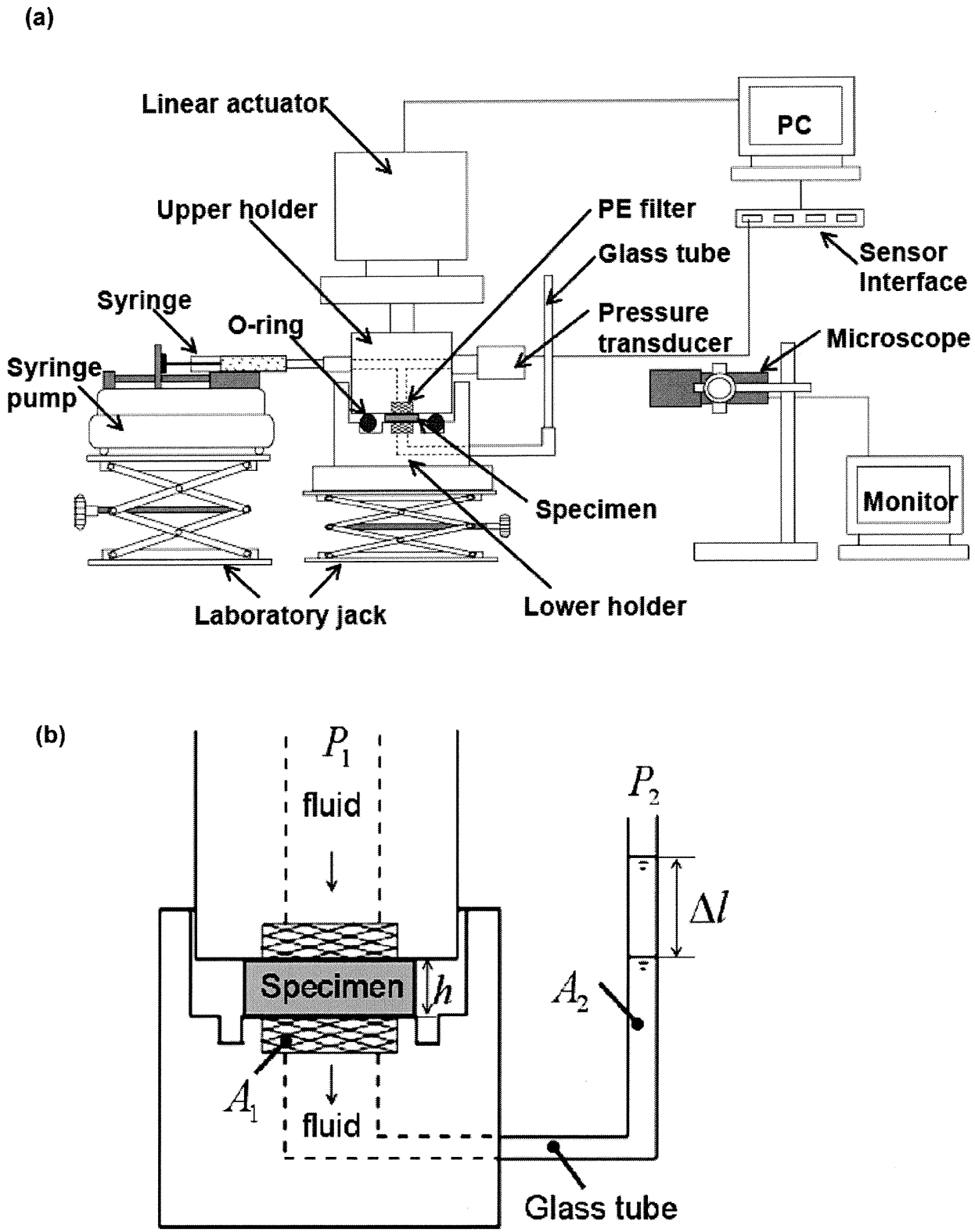

Fig. 2. Scheme of the device used for permeability testing. (a,b) Schematic drawing of the permeability testing apparatus used for assessment of cartilage layer-specimens. Sandwiched layer specimens of an initial thickness of h_0 was compressed with a strain of 30 % ($\varepsilon = 0.3$) in a saline solution at 37 °C. Under a hydrostatic pressure difference of 70 kPa (P_1-P_2), the outflow rate from the specimen $\Delta l/\Delta t$ was measured to determine the permeability of the specimen from the equation shown in the text, where A_1 represents the cross-sectional area of the specimen, while A_2 represents the cross-sectional area of the outflow capillary.

section was then further dehydrated in 70 % ethanol for 5 min and finally in 100 % ethanol for 5 min. Subsequently, it was fixed on a metal device and immersed in liquid nitrogen. SEM observation was performed for the specimens using a digital microscope (VE-8800, Keyence, Osaka, Japan) at an acceleration voltage of 1.5 kV and a magnification ratio of 15-700.

Atomic Force Microscopy observation and micro-indentation testing

An atomic force microscope (AFM) (Nanoscope IIIa, Veeco Instruments, Plainview, NY, USA) was used to examine structure-function relationships of uninjured cartilage and repaired tissues in the present study. AFM is a very high-resolution type of scanning probe microscopy, with demonstrated resolution on the order of fractions of a nm. It should be noted that not only geometry but also structural properties such as indentation stiffness can be obtained from uninjured cartilage and repair tissues without any specimen preparation (Kumar *et al.*, 2001; Fujie *et al.*, 2007; Nansai *et al.*, 2011).

Each cylindrical specimen (Uninjured cartilage; $n = 11$, TEC-treated tissue; $n = 7$, no-treated tissue; $n = 4$) was mounted on the sample stage of the AFM and soaked in saline solution at room temperature. Surface scanning was performed on the specimen using a contact mode of the AFM at a scan area of 30 x 30 μm and scan rate of 0.3 Hz using a silicon nitride probe (spring constant: 0.06 N/m, DNP-S, Veeco Instruments). From the obtained surface images, arithmetic surface roughness (R_a) was calculated using software installed in the AFM. Finally, a micro-indentation test was performed three times at 5 sites in each sample at an indentation rate of 5.12 μm/second and the values were averaged to determine the micro-scaled stiffness of the specimen. The distance between the sites assessed was always more than 1 mm. The stiffness of the superficial layer of uninjured cartilage and repair tissue, defined as the slope of the force-indentation curves between 300 and 400 nm of indentation, were subsequently obtained.

Friction testing

Reciprocal friction testing was performed for each cylindrical specimen using a friction tester developed in our laboratory (Ando *et al.*, 2007). The specimens were fixed to a probe edge of the tester so that the cartilage/cartilaginous repair tissue surface was uniformly attached to a glass plate soaked in saline solution at 37 °C. Sixty seconds after the application of vertical load of 1.76 N (140 kPa), the specimen was subjected to reciprocal friction at a rate of 20 mm/s with a stroke of 25 mm. Frictional force was measured with a custom-made cantilever-shaped load transducer with strain gauges having the rated output of 0.36 N and the non-linearity of 0.04 %. Coefficients of friction, defined as the ratio of frictional force to vertical load, were subsequently determined.

Permeability testing

For the permeability test, the cylindrical specimens used for the previous tests were transversely sliced to surface, middle, and deep layer specimens of approximately 300 μm in thickness, using a microtome. A permeability tester similar to that developed by Weiss *et al.* (Weiss *et al.*, 2006) was designed (Fig. 2ab). Each specimen of an initial thickness of h_0 was sandwiched between the top and bottom holders soaked in saline solution and then compressed with a strain of 30 % ($\varepsilon = 0.3$). A syringe pump was manually controlled for 1000 s so that the hydrostatic pressure difference P_1-P_2 was maintained at 70 kPa with a fluctuation of less than 2 kPa. The outflow rate from the specimen $\Delta l/\Delta t$ was measured and the permeability of the specimen, k was determined from the equation shown below based on Darcy's law (Mansour *et al.*, 1976), where A_1 represents the cross-sectional area of the specimen, while A_2 represents the cross-sectional area of the outflow capillary.

$$k = \frac{A_2 h_0 (1-\varepsilon)\Delta l}{A_1 (P_1 - P_2)\Delta t}$$

Note that no outflow was allowed from the lateral side of the specimen by means of an O-ring fixed into the tester around the specimen.

Statistical analysis

The results are presented as mean ± SD. In micro-indentation testing, friction testing, and permeability testing, the specimen numbers were 11 for uninjured cartilage, 7 for TEC-treated tissue and 4 for no-treatment repair tissue, and these results were analysed using analysis of variance (ANOVA) with Bonferroni's multiple comparison t-test in the STATVIEW version 5.5 software statistics package (SAS Institute, Cary, NC. USA). The results of the superficial thickness and histological scoring were analysed using unpaired t-tests and the Mann-Whitney U-test, respectively. Significance was set at $p < 0.05$.

Results

Overall histological and biomechanical evaluation of repair cartilage

When implanted with a TEC, the cartilage defects were repaired with a cartilaginous tissue with positive Safranin O staining in most of the repair tissue and such staining was also seen throughout the uninjured cartilage (Fig. 3ab). The untreated control defects were partially covered with a fibrous tissue with some evidence of osteoarthritic changes, associated with further loss of cartilage and erosion of subchondral bone (Fig. 3c). By O'Driscoll scoring, the TEC-mediated repair tissue had 62.5 % to 93.8 % values of the mean score of the uninjured cartilage in each category and the overall score was 18.1 ±3.7, which was 75.4 % of that of uninjured cartilage (score: 24) (Fig. 3d). For the histological scoring, all assessment criteria for the TEC-treated group were significantly higher than those for the untreated group, and also lower than that of uninjured group (Fig. 3d). The stress-strain relationships of the uninjured, TEC-treated and untreated specimens in the quasi-static compression test are shown in Fig. 3e. In the quasi-static compression test, the tangent modulus of the TEC-treated cartilage-like tissue was 1438.8 ±414.6 kPa,

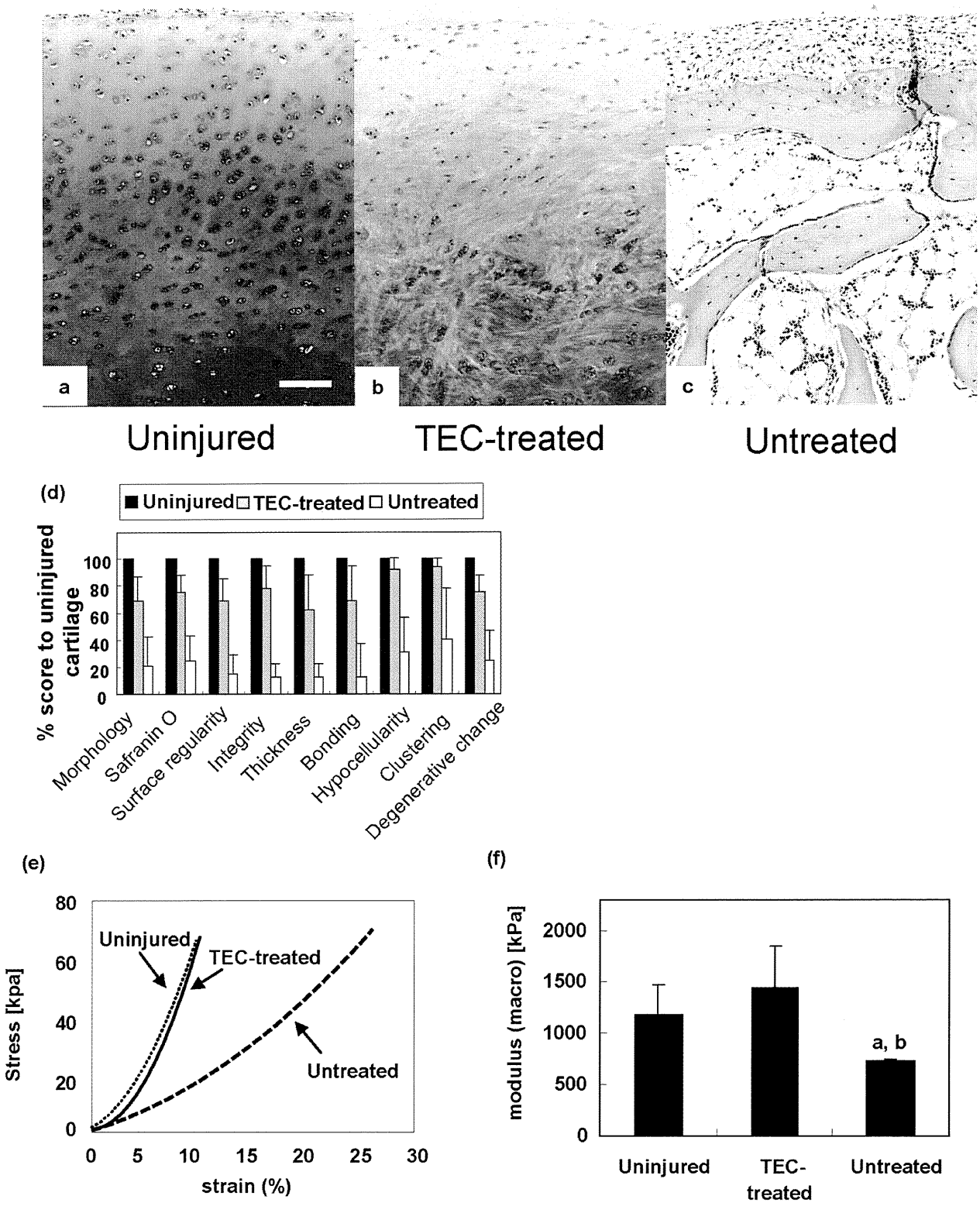

Fig. 3. Overall histological observations and biomechanical evaluation of TEC-mediated repair cartilage. **(a,b,c)** Safranin O staining of porcine uninjured normal articular cartilage **(a)** and chondral lesions treated with **(b)** or without **(c)** TEC at 6 months after implantation. Bar = 100 μm. **(d)** O'Driscoll histological and histochemical grading scale of uninjured articular cartilage (n = 12), repair tissue treated with (TEC; n = 8) and without treatment (Untreated; n = 4) TEC. **(e)** Typical stress-strain relationships of TEC-treated tissue compared with those of uninjured cartilage and untreated tissue. **(f)** Tangent modulus of uninjured cartilage (n = 10), the chondral lesion in the TEC treated group (n = 6) and those in the untreated group (n = 3) at compression rate of 4 μm/s. a: $p < 0.05$, compared to uninjured cartilage. b: $p < 0.05$ compared to the TEC treated group. There were no significant differences between the tangent modulus of TEC-mediated repair tissue and that of uninjured cartilage.

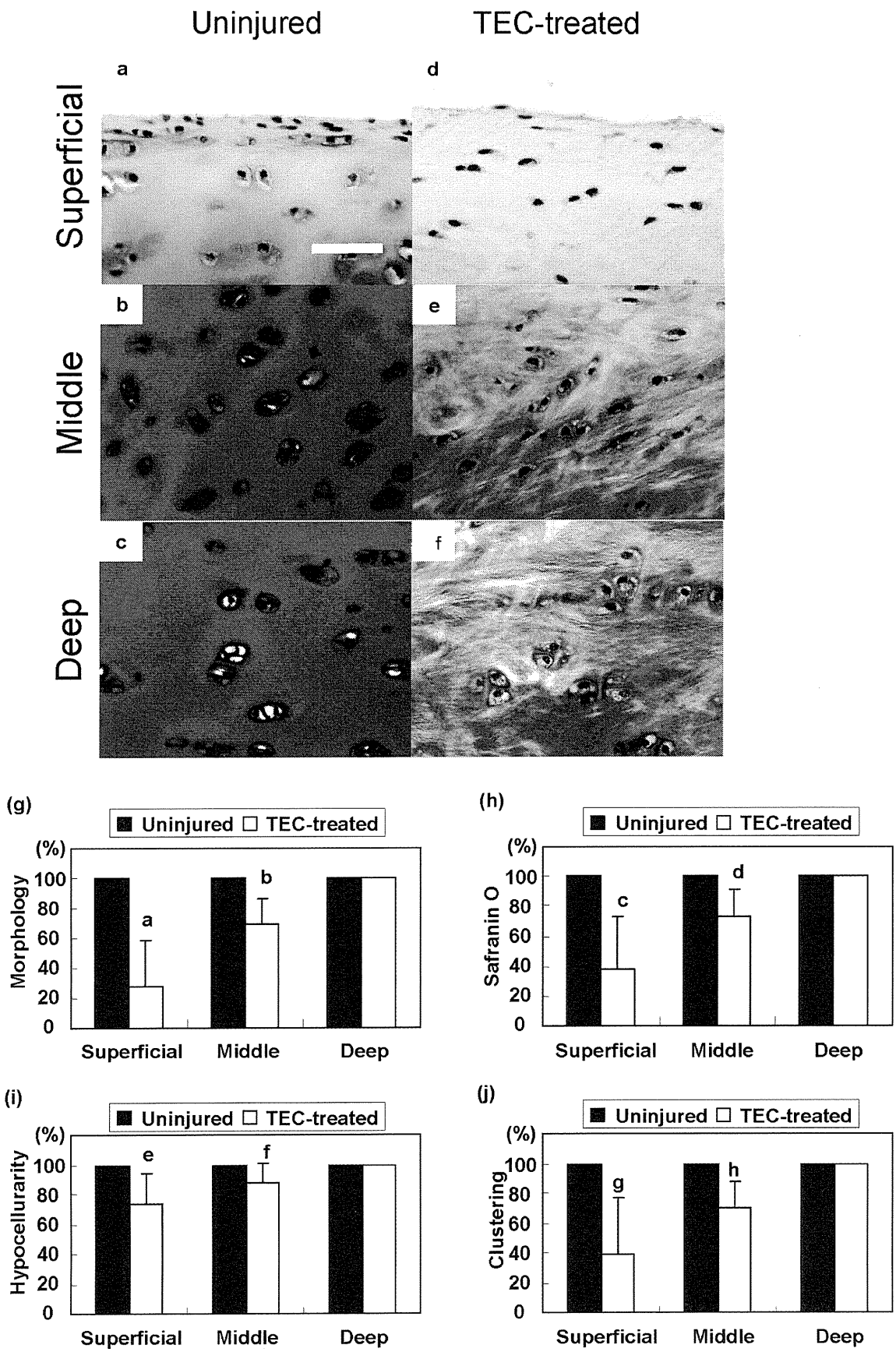

Fig. 4. Zonal histology of uninjured cartilage and the TEC-mediated repair cartilage. (a,b,c) Safranin O staining of superficial **(a)**, middle **(b)** and deep **(c)** zone of porcine chondral lesions 6 months after implantation of TECs. Bar = 25 μm. **(d,e,f)** Safranin O staining of superficial **(d)**, middle **(e)**, and deep **(f)** zone of uninjured cartilage. Bar = 25 μm. **(g,h,i,j)** Zonal histological and histochemical grading scale of uninjured articular cartilage and TEC-mediated repair tissue ($n = 8$). a,c,g: $p < 0.001$, b,d,h; $p < 0.01$, e,f; $p < 0.05$ compared to the uninjured cartilage.

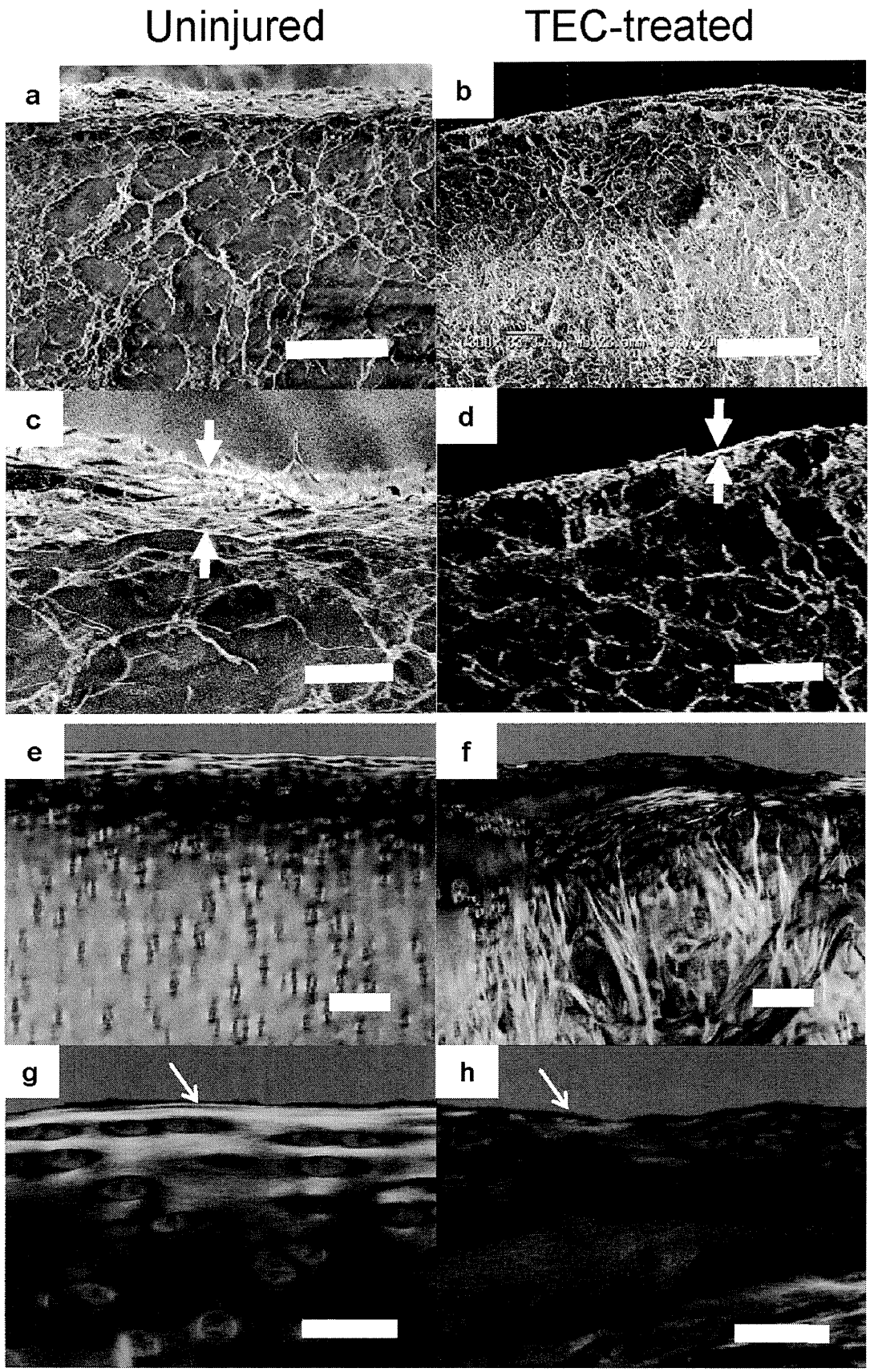

Fig. 5. Surface ultrastructure of repair cartilage. (a,b) Scanning electron microscopic (SEM) view of porcine normal **(a)** and chondral lesions treated with TEC at 6 months after implantation **(b)**. Bar = 100 μm. **(c,d)** Higher magnification SEM view of porcine uninjured cartilage (c) and chondral lesions treated with TEC (d). Bar = 25 μm. Arrow; the thickness of the superficial layer. **(e,f)** Polarised microscopic view of porcine uninjured (e) and chondral lesions treated with TEC (f). Bar = 200 μm. **(g,h)** Higher magnification polarised microscopic view of porcine uninjured (g) and chondral lesions treated with TEC (h). Bar = 50 μm. Arrows: one bright thin fibre was observed at the most superficial layer which has been termed the lamina splendens.

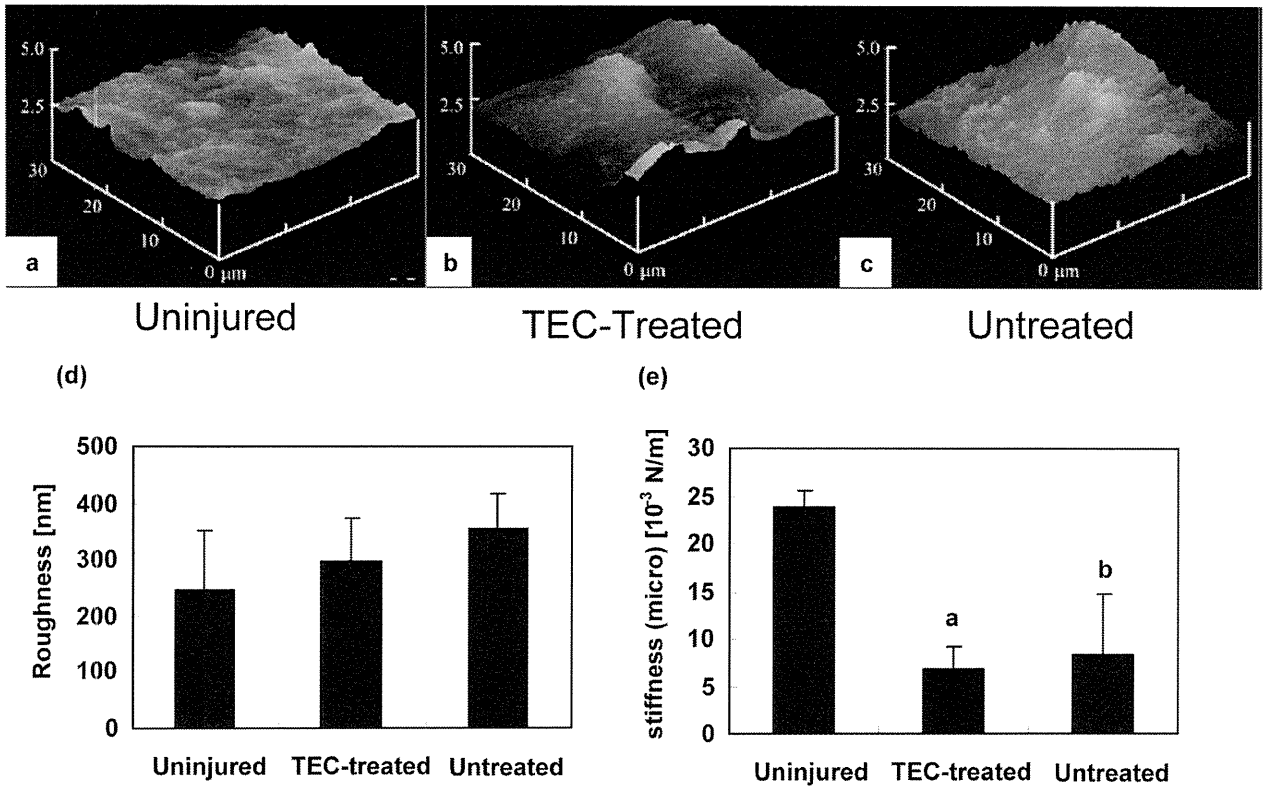

Fig. 6. Surface analysis of uninjured and TEC-mediated repair cartilage. (a,b,c) Atomic force microscopic (AFM)) view of porcine uninjured cartilage **(a)** and a chondral lesion treated with **(b)** or without **(c)** a TEC at 6 months after implantation. **(d)** The surface roughness of uninjured cartilage (n = 11), the chondral lesions in the TEC treated group (n = 7) and that in the untreated group (n = 4). **(e)** The surface stiffness of normal cartilage, the chondral lesions in the TEC treated group and that in the untreated group. a: $p < 0.05$, b: $p < 0.05$ compared to normal cartilage.

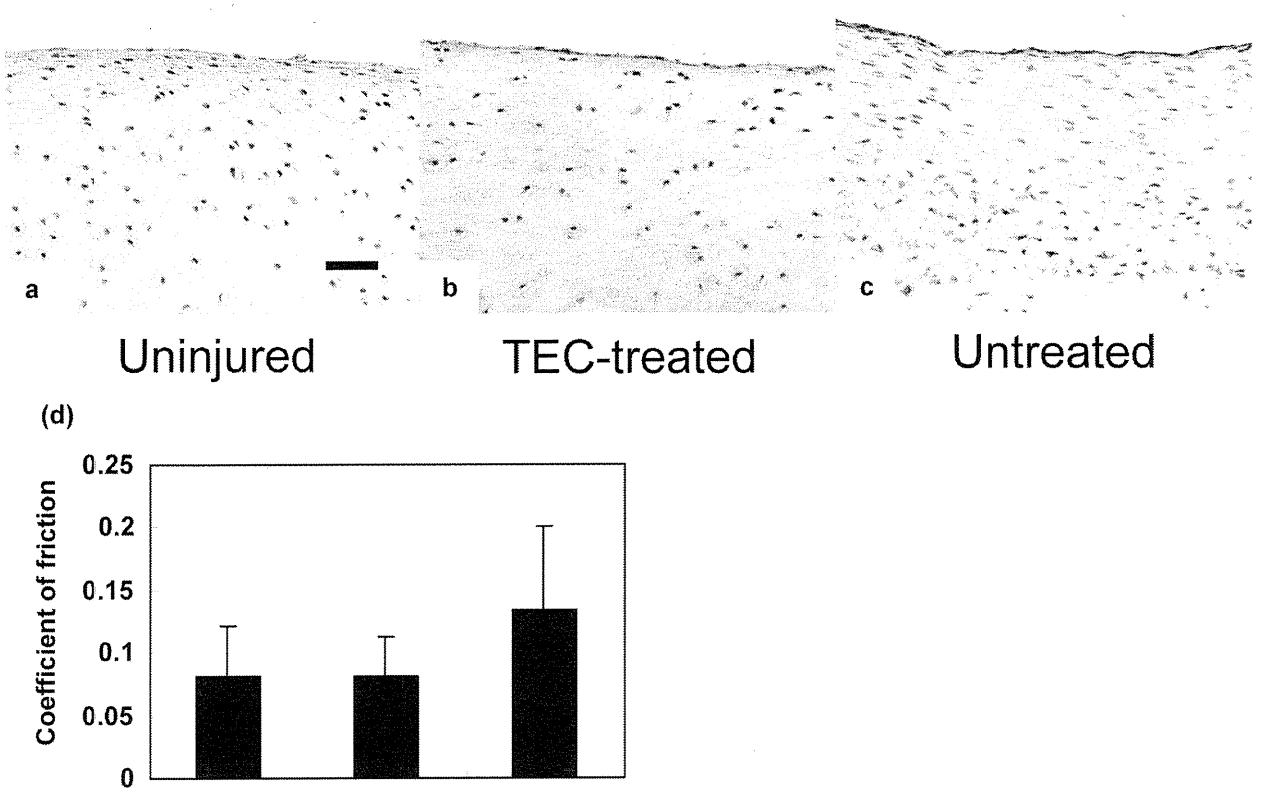

Fig. 7. Localisation of PRG4 in cartilage and lubrication properties. (a,b,c) Lubricin expression at the surface zone of uninjured **(a)** and chondral lesions treated with **(b)** or without **(c)** a TEC. **(d)** Frictional coefficient of uninjured cartilage (n = 11) and chondral lesions in the TEC treated group (n = 7) at 60 s with the application of a compressive force of 1.76 N. There were no significant differences between the frictional coefficients of repair tissue following implantation of a TEC and those of normal cartilage.

with no significant differences when compared to uninjured cartilage values (1182.0 ±297.0 kPa). In contrast, the tangent modulus of the untreated chondral defect tissue was 725.6 ±23.9 kPa, which was significantly lower than that of the TEC-treated cartilaginous tissue and uninjured cartilage (Fig. 3f).Thus, the TEC treated tissue had overall comparable values in morphology and biomechanical properties with those of uninjured cartilage.

Zonal histology of TEC-mediated repair cartilage

Zonal histological evaluation of the uninjured articular cartilage at higher magnification revealed that the most superficial area was a layer of fibrocartilage tissue lacking Safranin O staining (Fig. 4a). Most of the cartilage matrix beneath the fibrous layer was stained with Safranin O throughout the zones (Fig. 4abc). In the TEC-mediated repair cartilage, fibro-cartilaginous tissue was predominant in the superficial zone of the repair tissue lacking Safranin O staining (Fig. 4d) while most of the repair matrix in the middle and deep zones was composed of cartilaginous matrix with positive Safranin O staining (Fig. 4ef). By O'Driscoll histological scoring, the ratio of the score of the TEC-mediated repair tissue to that of uninjured cartilage was significantly lower in the superficial zone than in the middle and deep zone regarding the category of morphology, Safranin O staining, hypocellularity and chondrocyte clustering (Fig. 4ghij).

Surface ultrastructure of the TEC-mediated repair cartilage

SEM assessment revealed that there was a dense paralleled fibrous bundle at the most superficial layer of uninjured articular cartilage (Fig. 5a). Conversely, one thin layer covered the surface of the superficial zone of the TEC-mediated repair-cartilage (Fig. 5b). Higher magnification views revealed that the width of the dense paralleled fibrous bundle was approximately 20 μm. (Fig. 5c) while the one thin superficial layer of the TEC-mediated repair cartilage was approximately 2 μm (Fig. 5d). Picrosirius red staining revealed a bright orange band in the superficial layer of uninjured articular cartilage, of which the thickness was approximately 100-150 μm (Fig. 5e). It was notable that a red-coloured thin band with approximately 3 μm thickness was observed at the very surface of the orange band zone (Fig. 5g, arrow). Such a red band was not detected at the surface of the TEC-mediated repair tissue (Fig. 5f,h arrow).

Surface analysis of TEC-mediated repair cartilage

AFM analysis indicated that the surface of the uninjured cartilage consisted of bump-like protrusions of approximately 2 μm in height. The surface of the TEC-mediated and untreated cartilaginous tissues arising after injury exhibited a slightly rougher and a more irregular surface than that detected on uninjured cartilage (Fig. 6abc). The arithmetic surface roughness of the TEC-mediated cartilaginous tissue was 298 ±76.5 nm, which was a value between that of uninjured cartilage (247 ±103 nm) and the untreated cartilage-like tissue (354 ±61.7 nm), although no significant differences were detected between the three groups (Fig. 6d).

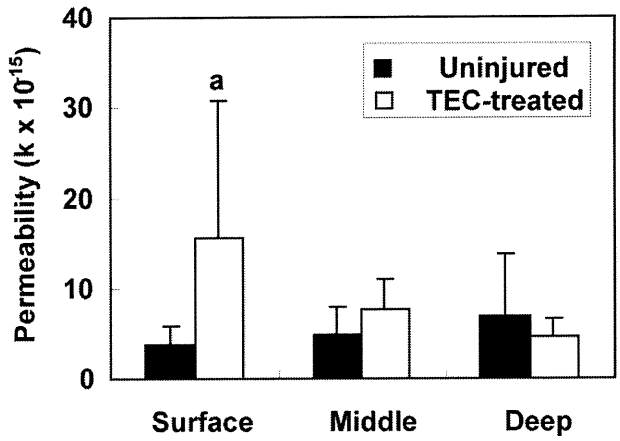

Fig. 8. TEC-mediated cartilage-like repair tissue exhibits low permeability at the superficial zone. Permeability of uninjured cartilage ($n = 11$) and chondral lesions in the TEC treated group ($n = 7$) at the surface, middle and deep zone. a: $p < 0.05$, compared to normal cartilage.

Micro-indentation testing showed that the surface stiffness of the TEC-mediated cartilaginous repair tissue was 6.79 ±2.30 x 10^{-3} N/m and the untreated cartilaginous tissues was 8.21 ±6.51 x 10^{-3} N/m, which were both significantly lower than values for uninjured cartilage (23.8 ±1.70 x 10^{-3} N/m) (Fig. 6e).

Localisation of PRG4 in TEC-mediated repair cartilage and lubrication properties

The proteoglycan 4 (PRG4) (lubricin) is considered to be the major protein responsible for the lubrication of articular cartilage (Swann *et al.*, 1977; Jay, 1992). PRG4 was localised to the surface of both uninjured and TEC-mediated repair cartilage, as well as the untreated repair tissue (Fig. 7abc). Friction testing indicated that the coefficient of friction for the TEC-mediated tissue was 0.081 ±0.033, with no significant differences observed between those of uninjured cartilage (0.081 ±0.041) and the untreated repair tissue (0.133 ±0.067) (Fig. 7b). The latter finding is likely due to the wide variability observed in the samples from the untreated group.

Permeability of the TEC-mediated repair cartilage

Permeability testing showed that the permeability of the TEC-mediated cartilage-like tissue was significantly higher than that of normal cartilage (18.6 ±15.7 x 10^{-15} m^4/Ns *vs.* 3.86 ±2.00 nm x 10^{-15} m^4/Ns) at the superficial zone, while there were no significant differences detected at the middle (6.63 ±3.26 x 10^{-15} m^4/Ns *vs.* 4.74 ±3.13 nm x 10^{-15} m^4/Ns) and the deep zones (4.67 ±2.00 x 10^{-15} m^4/Ns *vs.* 7.02 ±6.73 nm x 10^{-15} m^4/Ns) (Fig. 8). These results indicated that the middle to deep zones of the TEC-mediated repair cartilage had a fluid retention capacity similar to uninjured cartilage, while the superficial zone was more permeable than uninjured cartilage.